Self-Coherent Camera as a focal plane phasing sensor - Overview and early comparison with the Zernike Phase Contrast Sensor

P. Janin-Potiron[a], P. Martinez[a], P. Baudoz[b], and M. Carbillet[a]

[a]Laboratoire Lagrange, UMR7293, Université de Nice Sophia-Antipolis, CNRS, Observatoire de la Côte d´Azur, Parc Valrose, Bât. Fizeau, 06108 Nice Cedex 2, France
[b]LESIA, Observatoire de Paris, CNRS and University Denis Diderot Paris 7, 5 place Jules Janssen, 92195 Meudon, France

ABSTRACT

In order to achieve the high performance required for the astronomical science programs with coming Extremely Large Telescopes (ELTs), the errors due to segment misalignment must be reduced to tens of nm. Therefore the development of new co-phasing techniques is of critical importance for ground-based telescopes, and to a large extent for future space-based missions. We propose a new co-phasing method directly exploiting the scientific image delivered by the Self-Coherent Camera (SCC) by adequately combining segment misalignment estimators (piston and tip/tilt) and image processing. The Self-Coherent Camera Phasing Sensor (SCC-PS) is shown to be capable of estimating accurately and simultaneously piston and tip/tilt misalignments and to correct them in close-loop operation in a few iterations. By contrast to several phasing sensor concepts the SCC-PS does not require any a priori on the signal at the segment boundaries, or a dedicated optical path. The SCC-PS is a non-invasive concept that works directly on the scientific image of the instrument, either in a coronagrahic or a non-coronagraphic observing mode. The primary results obtained in this study are very promising and demonstrate that the SCC-PS is a serious candidate for segment co-phasing at the instrument level or at the telescope level for both ground- and space-based applications. Applications of the estimators and algorithm developed for the SCC-PS seem to be possible to other on-segment aberration measurement. Early studies are already in progress to adapt these processes.

Keywords: High angular resolution, ELTs, adaptive optics, closed-loop control

1. INTRODUCTION

Extremely Large Telescopes (ELTs) are considered as the next leap forward for ground-based observations. Their optical characteristics (primary diameter up to 39 meter diameter for the forthcoming E-ELT, the European ELT) will deliver unreached high resolution and sensitivity for new thrilling science observations, such as exoplanets direct imaging.

The size of the primary mirror and the observation capability of a telescope are nowadays bound up with each other. Segmented mirrors are necessary for the future exoplanet space-based projects for increasing the telescope size by benefiting from the limited room offered with a given launch vehicle. However, segmentation highly complicates the structure of the pupil. Tackling the various effects related to the segmentation of the primary mirror in order to achieve a certain level of the image quality is fundamental.[1,2] In particular, the most well-known issue is to achieve a smooth continuous mirror surface, a process known as co-phasing. The alignment of segments is mandatory as their misalignments are stochastic effects (the value of characteristics changed randomly from segment to segment) and produce speckles in the scientific image. A properly phased telescope will have a resolution comparable to the total diameter of the entire segmented primary mirror. Before phasing, a telescope will have very poor resolution limited by the diameter of an individual segment. While the

Further author information: (Send correspondence to Pierre Janin-Potiron)
Pierre Janin-Potiron: E-mail: Pierre.Janin-Potiron@oca.eu, Telephone: +33 (0)4 92 00 39 68

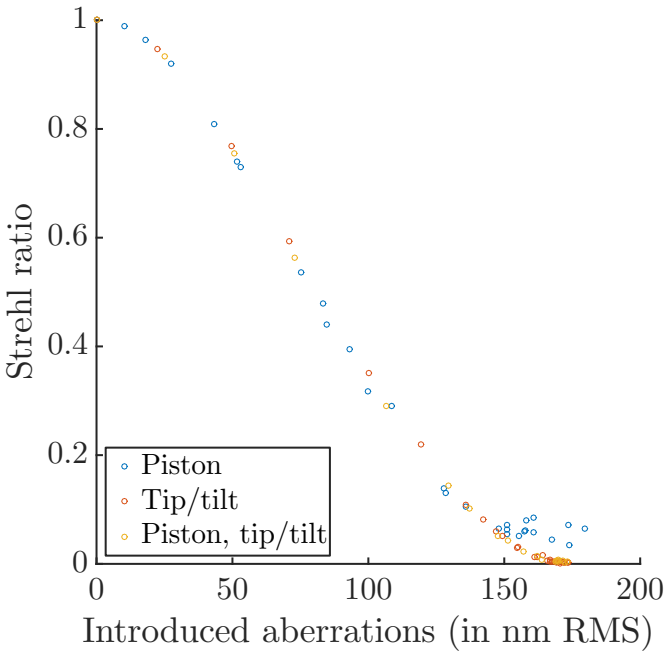

Figure 1. Strehl ratio in function of introduced aberrations. Blue dots: piston only aberrations; red dots: tip/tilt only aberrations; yellow dots: both piston and tip/tilt aberrations.

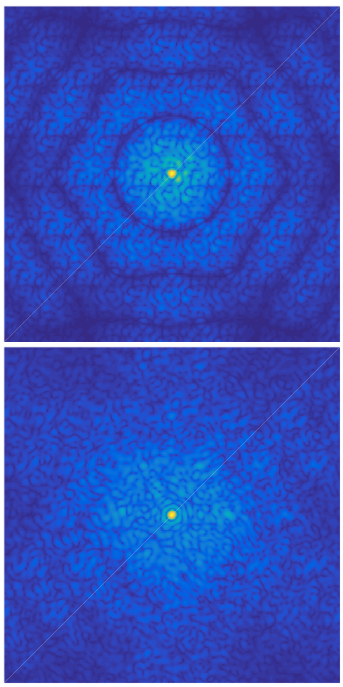

Figure 2. PSF of a segmented pupil for piston only aberrations (left) and tip/tilt only aberrations (right).

basic technologies required for co-phasing segmented telescopes have been demonstrated for few meter telescope diameters (e.g., Keck or Gran Telescopio Canarias observatories, James Web Space Telescope), ELTs represent a significant change in dimension and wavefront control strategies.

At the telescope level, the active optics system aims at maintaining the required shape and position of the segments. Conventional active optics co-phasing control loop requires several elements to operate: (1) position sensors located at the back or at the edge of each segment to provide relative positions of two adjacent segments; (2) actuators situated underneath each segment to compensate displacements between them; (3) phasing sensor to obtain the periodical measurement of absolute misalignment between segments. High performance and image quality require the primary mirror segments to be aligned at the level of few tens of nanometers, while the requirements of high-precision phasing for high contrast imaging instruments is still uncertain but might be much more demanding. That is why co-phasing the telescope's segments is of primary importance as we show just hereafter. We quantify the quality of the convergence by measuring the RMS value of the segments positions in the pupil plane. The Strehl ratio, S, can also be used to confirm the validity of the converging process. The expression linking S to the aberrations RMS value σ has been demonstrated[3] in case of piston error only and can be expressed as

$$S = \frac{1 + \exp(-\sigma^2)(N-1)}{N}. \tag{1}$$

If tip and tilt aberrations are added, no analytic formula is available. We present in Fig. 1 the behavior of the Strehl ratio with increasing RMS value for a 5-rings segmented mirror. We clearly see that for piston only, the Strehl ratio reaches a plateau when the introduced aberrations tend to large values. This is not the case when tip and tilt are added. Indeed, tip and tilt aberrations lead to the appearance of higher-order peaks in the telescope PSF[4] that are not limited in spatial range : one single segment can produce its own PSF anywhere in the focal plane depending on its tip and tilt aberrations level. In Fig. 2, the PSF of piston only and tip/tilt only aberrations are presented. Obviously, according to Eq. 1, the larger the number of segment the more the image quality will be affected.

In this context, several methods have been proposed to measure segment misalignments, where various co-phasing sensors are based on existing wavefront sensors usually employed in adaptive optics (AO) applications.

Co-phasing methods can be divided into three flavors: (1) pupil plane techniques such as the modified Shack-Hartmann,[5–7] the Mach-Zehnder interferometer[3,8,9] and avatars;[4,10] (2) intermediate plane techniques such as the curvature sensor;[11–13] (3) focal plane techniques such as the phase diversity,[14,15] Pyramid sensor.[16,17] More recent and peculiar approaches have been investigated using pupil asymmetry (asymmetric pupil wavefront sensor[18,19]), or differential optical transfer functions.[20]

P. Baudoz proposed a focal plane wavefront sensor called the Self-Coherent Camera[21] (SCC) exploiting the coherence of light to spatially encode the speckles in the detector plane. The SCC is capable of estimating accurately both phase and amplitude aberrations upstream of a coronagraph.[22] The present paper studies the use of the SCC as a cophasing sensor (restricted to the correction of the piston, tip and tilt errors). Piston errors represent segment vertical misalignments and tip/tilt errors represent the segment turned up or down at the inter-segment edges. The self-coherent camera phasing sensor (hereafter, SCC-PS) gathers several major advantages: by contrast to several phasing methods it does not require any a priori knowledge of the signal at the segment boundaries; the SCC-PS is an non-intrusive image plane technique (limited hardware and no dedicated optical path); and it works directly on the scientific image using a coronagraph or alternatively using a chop in diffractive component inserted in a filter wheel and used only during the primary mirror calibration. In addition, the SCC-PS will be presumably less sensitive to the so-called "island effect", consisting of the partial or complete coverage of the pupil by the dark zones created by the secondary mirror supports (the so-called spider arms), thus directly impacting a phasing sensor measuring the signal on the segment boundaries. Finally, the SCC-PS can be used as part of the active optics system of the telescope, or alternatively be directly inserted in the scientific instrument.

The paper reads as follows: in Sect. 2 we briefly recall the principle of the SCC and define the estimators we chose to measure the piston, tip and tilt on each segment and their reliability over the range of aberrations we introduce by means of numerical simulations. Then in Sect. 3 we discuss the performances of the convergence process. Results in term of reachable initial aberrations level are presented. Finally, in Sect. 4 we draw a first comparison between the SCC-PS and the Zernike Phase Contrast Sensor[4,10] (Zernike Unit for Segment phasing, ZEUS). These two phasing sensors will be tested on the Segmented Pupil Experiment for Exoplanet Detection[23] (SPEED) in order to assess their respective performances.

2. PRINCIPLE AND ESTIMATORS

The SCC was firstly developed[21] and used to spatially encode the speckles of a post-coronagraphic image in order to disentangle the signal between a star and a planet. It uses the coherence of light to produce interference pattern in the focal plane. With an adapted signal processing, one can easily retrieve the phase aberrations in the focal plane. We propose in this section to explain the SCC principle without entering the complex mathematical development and then to show how we use this method to retrieve the piston, tip and tilt errors in the focal plane of a segmented telescope.

2.1 Hardware principle

We follow Fig.3 to present the steps underlaying the SCC process. Full development can be found in previous[24] and coming[25] publications. Starting from the upper left of the diagram, as segments misalignment only introduce phase errors, we consider an incoming wavefront with only phase aberrations. Amplitude errors, that can result from island effect or gaps between segments, will be studied in a forthcoming work. The light is then focalized on a diffractive component. We put in our simulation a Four Quadrant Phase Mask (FQPM) to match the condition used in J. Mazoyer et al. study.[24] On the next pupil plane, a Lyot stop is placed as in a classical coronagraphic system but with an added pinhole (orange lines on Fig. 3, named hereafter the reference hole). Interferences between the central and reference holes occur in the detector plan. These fringes spatially encode the speckles and allow, after post-processing, to estimate the phase in the entrance pupil.

2.2 Post-processing and aberrations estimators

The post-processing uses only basic operations (i.e. multiplication and Fourier transform) and therefore is quite fast. At the end, we literally obtain a "copy" of the phase information in the entrance pupil. The full development can be found in publications[24,25] already mentioned earlier. Figure 4 presents the response of the system to

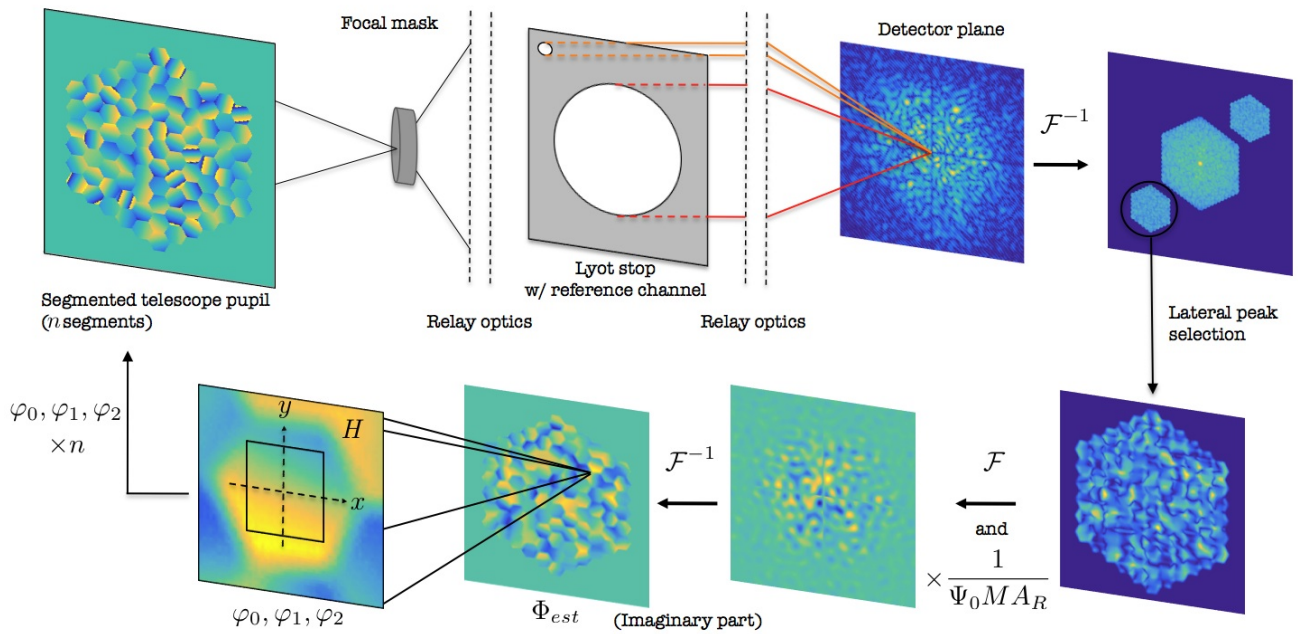

Figure 3. Illustration of the self-coherent camera phasing sensor (SCC-PS) principle. The red rays correspond to the path of the light in a classical coronagraph propagation process. The orange rays correspond to the path of light in the reference pupil in the Lyot stop. From the estimated phase map (ϕ_{est}) three estimators are evaluated on each segment (φ_0, φ_1, and φ_2).

piston, tip and tilt poke (from left to right respectively). Given this information, three estimators naturally comes to mind to quantify piston, tip and tilt. We define on each segment of Φ_{est} (see Fig. 3 for notations) a square zone (H) of side length h centered on the segment position (see Fig. 3 for notations). For piston, we calculate the integral of the signal over H and define

$$\varphi_0 = \iint_H \Phi_{est} \mathrm{d}x\mathrm{d}y. \tag{2}$$

For the estimation of the tip and tilt, the gradient of the signal ϕ_{est} is estimated following the $\boldsymbol{x}$ and $\boldsymbol{y}$ axis respectively (as defined on Fig. 4), and the estimators φ_1 and φ_2 are given by

$$\varphi_1 = \iint_H \nabla_x \left(\phi_{est}\right) \mathrm{d}x\mathrm{d}y, \tag{3}$$

$$\varphi_2 = \iint_H \nabla_y \left(\phi_{est}\right) \mathrm{d}x\mathrm{d}y, \tag{4}$$

where ∇_x and ∇_y stand for the gradient in the direction x and y respectively. In the case of piston (Fig. 5, left), the estimated phase is as expected λ-periodic and the limitation in the reachable bijective zone is as demonstrated[4,26] before, limited from $-\lambda/4$ to $\lambda/4$, the so-called π-ambiguity problem that appears in all phasing-sensor operating in monochromatic light. Outside this capture range, the position measurements are incorrect and lead, in some cases, to a situation where some segments will be shifted by the integer of the wavelength (this will be discussed in Sec. 3.2) instead of being phased to the zero step. The tip/tilt estimator exhibits somehow a larger capture range from $-3\lambda/8$ to $3\lambda/8$ (Fig. 5, right), which is nearly the same bijective zone (from about $-5\lambda/12$ to $5\lambda/12$) presented in Yaitskova et al.[9] (Fig. 12b of that paper).[27]

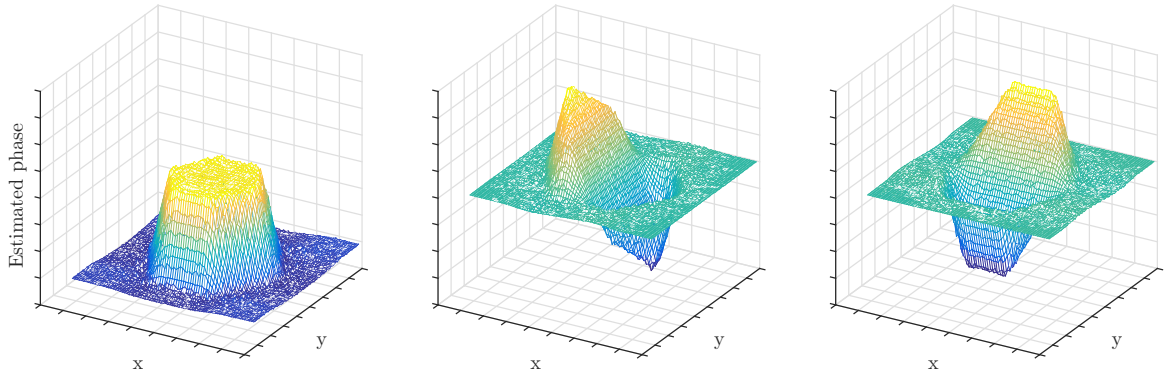

Figure 4. Estimated phase in the pupil plane after reconstruction for piston only (left), tip only (middle) and tilt only (right).

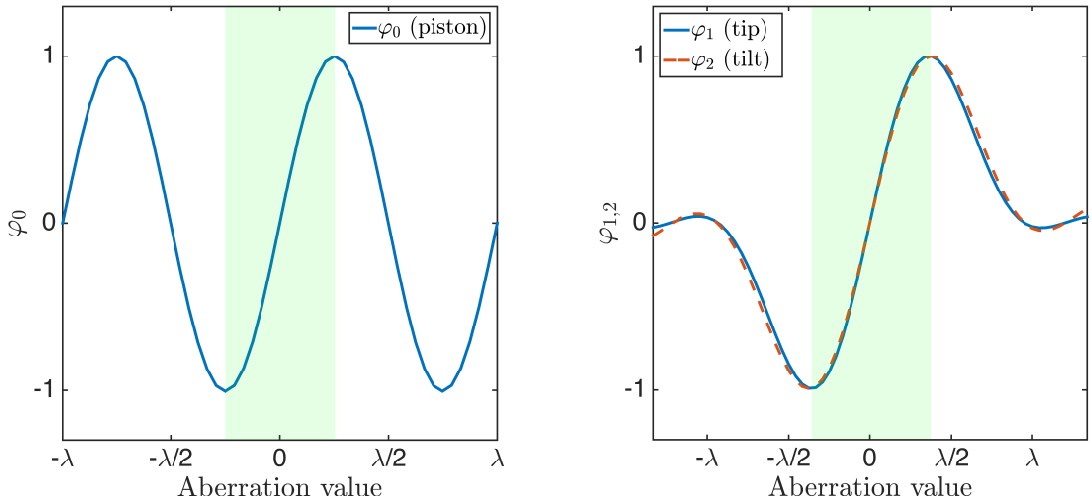

Figure 5. Representation of measured estimators (normalized) as function of the introduced aberration value for piston (left) and for tip/tilt (right). Green zones represent the capture range of the sensor. In this case, $h \simeq 23\%$ of segment's flat-to-flat distance.

3. ITERATION PROCESS

In this section, we present the parameters we use in our simulation, for example the mirror size, number of segment or sampling frequency. In a second time, we show the results of our phasing algorithm based on the residual RMS measurement, for both piston and tip/tilt aberrations.

3.1 Numerical assumptions

Simulations assume a segmented hexagonal entrance pupil composed of 91 segments of 50 pixels width (corner to corner) over 5 hexagonal rings without any central obscuration, nor secondary mirror supports as shown in Fig. 3. We make use of simple Fraunhofer propagators between pupil and image planes, that are implemented as fast Fourier transforms (FFTs) generated with a Matlab code. The telescope pupil is roughly 500 pixels diameter and the matrix are of dimensions 4096×4096 pixels. The resulting sampling in the focal plane is about 8 pixels per λ/D where D is the entrance pupil diameter. We assume a turbulence-free system (no dynamical aberrations) that is consistent with a spatial application, or representative of a ground-based application where the presence of a first stage consisting of an extreme AO system has already and ideally corrected the dynamical turbulence. We also assume a system free of aberrations with spacial frequency inferior to the segment size. We use a monochromatic light centered at 600 nm.

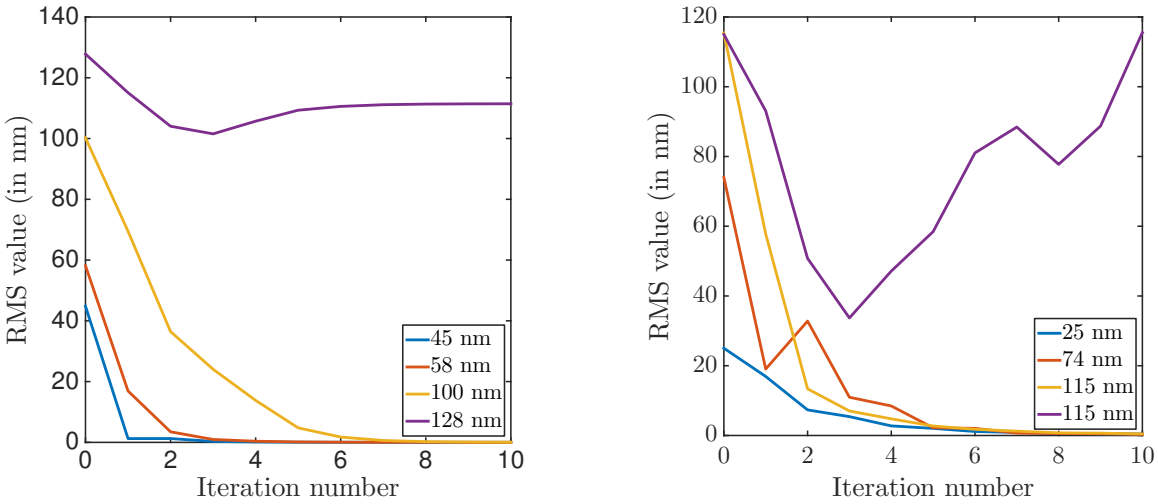

Figure 6. RMS value evolution of the aberrations over the pupil as function of the iteration number in the case of piston aberrations only (left) and for piston and tip/tilt (right). The starting RMS values are given in the captions.

3.2 System initialisation and closed-loop accuracy

We present in this section the results obtained with a closed-loop algorithm applied to an initially misaligned segmented telescope. The initialization follows two steps: (1) a segmented pupil is created. Random piston, tip and tilt aberrations, issued from a normal distribution with a zero mean and a σ standard deviation, $\mathcal{N}(0, \sigma^2)$, are introduced on each segment; (2) a calibration matrix is build actioning successively the segments in piston, tip and tilt. For each poke introduced on one segment, φ_0, φ_1 and φ_2 are measured on every segments and stocked in the calibration matrix. We obtain a square matrix with dominant diagonal terms. This converging process is adapted from a classical adaptive optic scheme.

A closed-loop iteration process is then repeated until convergence. It consists in two steps: (1) estimators φ are measured on each segment of the misaligned pupil image, produced with the SCC-PS; (2) system is inverted and estimated piston, tip and tilt are applied as a correction.

We independently analyze the convergence and the residual RMS in two cases: first with piston only, and then with both piston and tip/tilt. Figure 6 (left) presents the residual mirror RMS as function of the iteration number for various initial piston RMS only, whereas Fig. 6 (right) shows the residual RMS as function of the iteration number for various initial combination of piston and tip/tilt RMS. In both cases and as expected the results of the phasing strictly depends on the initial RMS. We have three possible outcomes: (1) the correction converges to 0 if the initial RMS is within the capture range of the SCC-PS; (2) the correction converges to a non-zero value for piston only as seen on Fig. 6 (left, purple curve); and (3) the correction diverges otherwise. In case (1), the correction is ideal. The residual RMS is then nearly null and the estimated Strehl ratio is roughly 100%. Quantitatively, it is remarkable that the convergence requires so few iterations. We compared our results to the results[9] obtained in a monochromatic regime at 500 nm (we use 600 nm), and the converge gain is obvious. For instance, considering piston only with an initial RMS of $\sim \lambda/10$, the SCC-PS requires less iterations to converge to a steady state. When piston and tip/tilt are considered together, the SCC-PS converges for higher initial aberration levels. Case (2) presents an effect known as the "λ-ambiguity", where part of the segments are positioned to a multiple of the wavelength from the ground level. Its effect is highly visible on the RMS values but it leads however to a Strehl ratio of roughly 100%. Case (3) occurs only in piston and tip/tilt simulations. When the system diverges, the residual RMS start fluctuating without any predictible pattern as seen on Fig. 6 (right, purple curve). (1) a calibration matrix is build, actioning every segment of the telescope in both piston, tip and tilt and measuring respectively the corresponding estimators (as presented in Sec. 2.2). This process is done once for each configuration, assuming a noise-free system; (2) random piston, tip and tilt, following a normal distribution $\mathcal{N}(0, \sigma^2)$, is then applied on a segmented pupil; (3) φ_0, φ_1 and φ_2 are measured for each segment and vectorized. Inverted calibration matrix is applied, and we end up with estimated piston, tip and

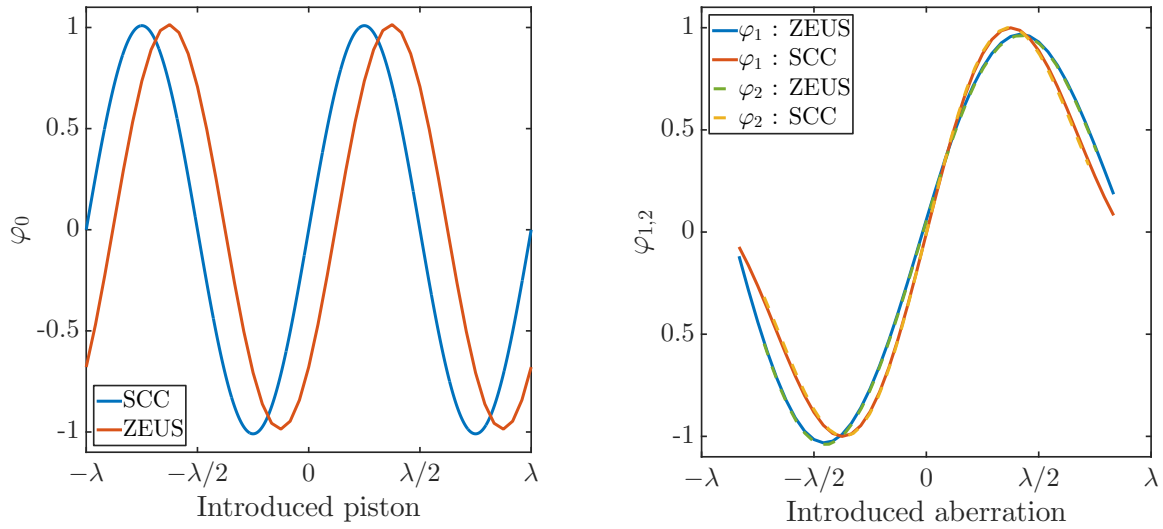

Figure 7. SCC and ZEUS normalized estimators in function of introduced aberrations, for piston only (left) and for tip and tilt only (right).

tilt for each segment; (4) the aberrations are finally corrected subtracting the estimated values to the current ones. (5) a closed loop is initiated and the process repeat until convergence.

4. EARLY COMPARISON WITH AN ON-SEGMENT ZEUS AND FUTURE IMPLEMENTATION ON SPEED

The above-mentioned ZEUS is based on a pupil plane analysis. A focal phase mask filtering is preformed to "reproduce" a Mach-Zehnder interferometer in order to provide a reliable co-phasing sensor. The major advantage lies on the ease of alignment of a focal mask compared to the two arms of an interferometer. In previous studies,[3,4] differential measurement of piston, tip and tilt estimators are computed across each intersegment. We performed numerical simulations using the ZEUS intersegment measurement,[27] and while piston only processes are perfectly handled, additional tip and tilt aberrations lead to not fully satisfactory results. It is in agreement with results proposed by other studies. Moreover, this method has the disadvantage to be influenced by the island effect or the gaps between segments. The SCC-PS has been shown to be a good candidate to correct the piston, tip and tilt misalignment over segmented pupils.[25] It provides an on-segment measurement and allows to look down upon the intersegment processing. As it is based on focal plane analysis, it is by principle insensitive to pupil shear and it does not require any pupil registration.[28,29]

In Sec. 2.2, we defined three estimators (φ_0, φ_1 and φ_2) that can be used for on-segment aberrations measurement. The closed-loop stage, presented earlier in Sec. 3.2, can then be applied as it is. Results obtained with ZEUS on an optical bench[30] (this conference) show similarities with the SCC-PS regarding the system response to piston, tip and tilt pokes. It would mean an on-segment measurement using previously developed technic should then be possible. Figure 7 presents a comparison between φ estimators measured for piston (left) and tip and tilt (right), for both SCC-PS and ZEUS. The same behavior in the three estimators is clearly observed. This is just a premise as an exhaustive and rigorous comparison will be done on SPEED.[23] For piston, we retrieve a bijective zone from $-\lambda/8$ to $3\lambda/8$ (a $\lambda/2$ width corresponding to the so-called "π-ambiguity"[26,31]). A shift along horizontal axis is however visible for ZEUS measurement. No further investigations have been done in our simulations, but on-bench measurement released by N'Diaye et al.[32] present the same horizontal displacement (Fig. 2 of this paper, for a ZEUS mask with a $\lambda/4$-OPD). It would mean that this phenomenon is inherent to ZEUS. For tip and tilt aberrations, there is a difference in the reachable bijective zone. For ZEUS, the length of the bijective zone is $\sim 0.9\lambda$ while for the SCC-PS, it gets closer to $3\lambda/4$. As the same parameters (position and size of zone H, same estimators) are used to perform the measurements, there must be an intrinsic behavior specific to each method that remain to be studied.

Early numerical comparisons between the SCC-PS and the on-segment ZEUS shows similarities when measuring φ estimators. It is likely that the closed-loop algorithm of the SCC-PS can be adapted to a ZEUS measurement and this will be tested in the next months on the SPEED bench. An ambivalent optical medium will allow both SCC-PS and ZEUS measurement and precise comparison will be made. The impact of the pupil discontinuities will also be addressed for real observation conditions (gaps, secondary supports, etc).

5. CONCLUSION AND FUTURE WORK

We show that the SCC-PS is able to estimate both piston and tip/tilt aberrations with fairly good accuracy. In a monochromatic and turbulence-free regime, the SCC-PS can correct in piston and tip/tilt a misaligned segmented pupil until $\sim \lambda/6$ RMS starting aberrations. The simulations converge to a steady-state where residual RMS values are close to zero and Strehl ratios close to 100%. Compared to an intersegment measurement with ZEUS, the SCC-PS provides faster convergence and higher acceptable starting RMS values. Other pros, such as insensitivity to pupil shear or intersegment gaps make of the SCC-PS a powerful solution to co-phase segmented telescopes. Meanwhile, the extension of the capture range of the SCC-PS using multi-reference holes at different wavelengths, as well as the ability of the concept to properly operate in the presence of the atmospheric turbulence, and sky coverage, still have to be studied. Finally, other diffractive components than the FQPM will be tested, and in particular optimal solutions (either coronagraphic or non-coronagraphic components) will be investigated. The SCC-PS is an attractive candidate for phasing segments in the vicinity of the ELT area and future coronagraphic space missions.

Implementations of the SPEED bench will start in February 2016. Parts composing the visible path (which is dedicated to the phasing process) are already in house. The camera has been characterized and a 169-segments deformable mirror from IrisAO is fully controllable in piston and tip/tilt. SPEED will include pupil and focal plane analysis. Comparison between them are soon to be made and emerging results will be presented in forthcoming publications.

ACKNOWLEDGMENTS

P. Janin-Potiron is grateful to Airbus Defense and Space (Toulouse, France) and the Région PACA (Provence Alpes Côte d´Azur, France) 2014 PhD program for supporting his PhD fellowship.

REFERENCES

[1] Yaitskova, N., Dohlen, K., and Dierickx, P., "Analytical study of diffraction effects in extremely large segmented telescopes," *Journal of the Optical Society of America A* **20**, 1563–1575 (Aug. 2003).

[2] Troy, M., Crossfield, I., Chanan, G., Dumont, P., Green, J. J., and Macintosh, B., "Effects of diffraction and static wavefront errors on high-contrast imaging from the thirty meter telescope," in [*Society of Photo-Optical Instrumentation Engineers (SPIE) Conference Series*], *Society of Photo-Optical Instrumentation Engineers (SPIE) Conference Series* **6272**, 2 (June 2006).

[3] Yaitskova, N., Dohlen, K., Dierickx, P., and Montoya, L., "Mach-Zehnder interferometer for piston and tip-tilt sensing in segmented telescopes: theory and analytical treatment," *Journal of the Optical Society of America A* **22**, 1093–1105 (June 2005).

[4] Surdej, I., *Co-phasing segmented mirrors : theory, laboratory experiments and measurements on sky*, theses (July 2011).

[5] Chanan, G. A., "Design of the Keck Observatory alignment camera," in [*Precision Instrument Design*], Bristow, T. C. and Hatheway, A. E., eds., *Society of Photo-Optical Instrumentation Engineers (SPIE) Conference Series* **1036**, 59 (May 1989).

[6] Chanan, G. A., Troy, M., and Ohara, C. M., "Phasing the primary mirror segments of the Keck telescopes: a comparison of different techniques," in [*Optical Design, Materials, Fabrication, and Maintenance*], Dierickx, P., ed., *Society of Photo-Optical Instrumentation Engineers (SPIE) Conference Series* **4003**, 188–202 (July 2000).

[7] Mazzoleni, R., Gonté, F., Surdej, I., Araujo, C., Brast, R., Derie, F., Duhoux, P., Dupuy, C., Frank, C., Karban, R., Noethe, L., and Yaitskova, N., "Design and performances of the Shack-Hartmann sensor within the Active Phasing Experiment," in [*Society of Photo-Optical Instrumentation Engineers (SPIE) Conference Series*], *Society of Photo-Optical Instrumentation Engineers (SPIE) Conference Series* **7012**, 3 (July 2008).

[8] Montoya-Martinez, L., *Application of Mach-Zehnder interferometer for co-phasing extremely large telescopes*, theses (Oct. 2004).

[9] Yaitskova, N., Montoya-Martinez, L., Dohlen, K., and Dierickx, P., "A Mach-Zehnder phasing sensor for extremely large segmented telescopes: laboratory results and close-loop algorithm," in [*Ground-based Telescopes*], Oschmann, Jr., J. M., ed., *Society of Photo-Optical Instrumentation Engineers (SPIE) Conference Series* **5489**, 1139–1151 (Oct. 2004).

[10] Dohlen, K., Langlois, M., Lanzoni, P., Mazzanti, S., Vigan, A., Montoya, L., Hernandez, E., Reyes, M., Surdej, I., and Yaitskova, N., "ZEUS: a cophasing sensor based on the Zernike phase contrast method," in [*Society of Photo-Optical Instrumentation Engineers (SPIE) Conference Series*], *Society of Photo-Optical Instrumentation Engineers (SPIE) Conference Series* **6267**, 34 (June 2006).

[11] Chanan, G., Troy, M., and Sirko, E., "Phase Discontinuity Sensing: A Method for Phasing Segmented Mirrors in the Infrared," *Appl. Opt.* **38**, 704–713 (Feb. 1999).

[12] Cuevas, S., Orlov, V. G., Garfias, F., Voitsekhovich, V. V., and Sanchez, L. J., "Curvature equation for a segmented telescope," in [*Optical Design, Materials, Fabrication, and Maintenance*], Dierickx, P., ed., *Society of Photo-Optical Instrumentation Engineers (SPIE) Conference Series* **4003**, 291–302 (July 2000).

[13] Chueca, S., Reyes, M., Schumacher, A., and Montoya, L., "DIPSI: measure of the tip-tilt with a diffraction image phase sensing instrument," in [*Society of Photo-Optical Instrumentation Engineers (SPIE) Conference Series*], *Society of Photo-Optical Instrumentation Engineers (SPIE) Conference Series* **7012**, 13 (July 2008).

[14] Lofdahl, M. G., Kendrick, R. L., Harwit, A., Mitchell, K. E., Duncan, A. L., Seldin, J. H., Paxman, R. G., and Acton, D. S., "Phase diversity experiment to measure piston misalignment on the segmented primary mirror of the Keck II Telescope," in [*Space Telescopes and Instruments V*], Bely, P. Y. and Breckinridge, J. B., eds., *Society of Photo-Optical Instrumentation Engineers (SPIE) Conference Series* **3356**, 1190–1201 (Aug. 1998).

[15] Delavaquerie, E., Cassaing, F., and Amans, J.-P., "Focal-plane wavefront sensing for segmented telescope," in [*Adaptative Optics for Extremely Large Telescopes*], 5018 (2010).

[16] Esposito, S., Pinna, E., Puglisi, A., Tozzi, A., and Stefanini, P., "Pyramid sensor for segmented mirror alignment," *Optics Letters* **30**, 2572–2574 (Oct. 2005).

[17] Pinna, E., Quiros-Pacheco, F., Esposito, S., Puglisi, A., and Stefanini, P., "The Pyramid Phasing Sensor (PYPS)," in [*Society of Photo-Optical Instrumentation Engineers (SPIE) Conference Series*], *Society of Photo-Optical Instrumentation Engineers (SPIE) Conference Series* **7012**, 3 (July 2008).

[18] Martinache, F., "The Asymmetric Pupil Fourier Wavefront Sensor," *PASP* **125**, 422–430 (Apr. 2013).

[19] Pope, B., Cvetojevic, N., Cheetham, A., Martinache, F., Norris, B., and Tuthill, P., "A demonstration of wavefront sensing and mirror phasing from the image domain," *MNRAS* **440**, 125–133 (May 2014).

[20] Codona, J. L. and Doble, N., "James Webb Space Telescope segment phasing using differential optical transfer functions," *ArXiv e-prints* (Feb. 2015).

[21] Baudoz, P., Boccaletti, A., Baudrand, J., and Rouan, D., "The Self-Coherent Camera: a new tool for planet detection," in [*IAU Colloq. 200: Direct Imaging of Exoplanets: Science and Techniques*], Aime, C. and Vakili, F., eds., 553–558 (2006).

[22] Mazoyer, J., *High-contrast direct imaging of exoplanets and circumstellar disks: from the self-coherent camera to NICI data analysis*, theses, Paris 7 (Sept. 2014).

[23] Martinez, P., Preis, O., Gouvret, C., Dejonghe, J., Daban, J.-B., Spang, A., Martinache, F., Beaulieu, M., Janin-Potiron, P., Abe, L., Fantei-Caujolle, Y., Mattei, D., and Ottogalli, S., "SPEED: the segmented pupil experiment for exoplanet detection," in [*Society of Photo-Optical Instrumentation Engineers (SPIE) Conference Series*], *Society of Photo-Optical Instrumentation Engineers (SPIE) Conference Series* **9145**, 4 (July 2014).

[24] Mazoyer, J., Baudoz, P., Galicher, R., Mas, M., and Rousset, G., "Estimation and correction of wavefront aberrations using the self-coherent camera: laboratory results," *A&A* **557**, A9 (Sept. 2013).

[25] Janin-Potiron, P., Martinez, P., Baudoz, P., and Carbillet, M., "Self-coherent camera as a focal plane wavefront sensor," *A&A* (In prep.).

[26] Vigan, A., Dohlen, K., and Mazzanti, S., "On-sky multiwavelength phasing of segmented telescopes with the Zernike phase contrast sensor," *Appl. Opt.* **50**, 2708 (June 2011).

[27] Janin-Potiron, P., *Développement d'une unité de phasage pour télescope à pupille segmentée*, Master's thesis, Université Joseph Fourier, Grenoble I, Pierre.Janin-Potiron@oca.eu (June 2014).

[28] Surdej, I., Koenig, E., Yaitskova, N., and Vandame, B., "APE segment pattern recognition in new phasing techniques," in [*Society of Photo-Optical Instrumentation Engineers (SPIE) Conference Series*], *Society of Photo-Optical Instrumentation Engineers (SPIE) Conference Series* **6267**, 38 (June 2006).

[29] Surdej, I., Lorch, H., Noethe, L., Yaitskova, N., and Karban, R., "Pattern recognition and signal analysis in a Mach-Zehnder type phasing sensor," in [*Society of Photo-Optical Instrumentation Engineers (SPIE) Conference Series*], *Society of Photo-Optical Instrumentation Engineers (SPIE) Conference Series* **6696**, 0 (Sept. 2007).

[30] Galland, N., El Hadi, K., Sauvage, J. F., Dohlen, K., Fusco, T., Marchis, F., and N'Diaye, M., "Coupling of wfs with a segmented dm test of different concepts: Sh, pyramid, zernike phase sensor," (October 2015).

[31] Surdej, I., Yaitskova, N., and Gonte, F., "On-sky performance of the Zernike phase contrast sensor for the phasing of segmented telescopes," *Appl. Opt.* **49**, 4052 (July 2010).

[32] N'Diaye, M., Dohlen, K., Caillat, A., Costille, A., Fusco, T., Jolivet, A., Madec, F., Mugnier, L., Paul, B., Sauvage, J.-F., Soummer, R., Vigan, A., and Wallace, J. K., "Design optimization and lab demonstration of ZELDA: a Zernike sensor for near-coronagraph quasi-static measurements," in [*Society of Photo-Optical Instrumentation Engineers (SPIE) Conference Series*], *Society of Photo-Optical Instrumentation Engineers (SPIE) Conference Series* **9148**, 91485H (Aug. 2014).